

Ultrasound-modulated optical tomography of absorbing objects buried in dense tissue-simulating turbid media

Lihong Wang and Xuemei Zhao

Continuous-wave ultrasonic modulation of scattered laser light was used to image objects buried in tissue-simulating turbid media. The buried object had an absorption coefficient greater than the background turbid medium. The ultrasonic wave that was focused into the turbid media modulated the laser light that passed through the ultrasonic field. The modulated laser light that was collected by a photomultiplier tube reflected the local mechanical and optical properties in the zone of ultrasonic modulation. Objects buried in the middle plane of 5-cm-thick dense turbid media were imaged with millimeter resolution through the scanning and detecting alterations of the ultrasound-modulated optical signal. The optical properties of the dense turbid media included an absorption coefficient of 0.1 cm^{-1} and a reduced scattering coefficient of 10 cm^{-1} and were comparable with those of biological tissues in the visible and near-IR ranges. The dependence of the ultrasound-modulated optical signal on the off-axis distance of the detector from the optic axis and the area of the detector was studied as well.

© 1997 Optical Society of America

Key words: Ultrasonic modulation, acousto-optics, optical imaging, optical tomography, turbid media.

1. Introduction

Nonionizing optical tomography of biological tissues, including breast tissues, has been an active research field.¹ The contrast mechanism of optical imaging is based on the difference in optical properties between diseased and surrounding normal biological tissues. Several techniques that are being investigated include time-gated optical imaging, time-resolved optical imaging, frequency-domain optical imaging, and optical coherence tomography. The time-resolved and frequency-domain techniques are mathematically linked by Fourier transform and have achieved comparable results, namely, a resolution of several millimeters for approximately 5-cm-thick tissues or tissue phantoms. Optical coherence tomography has achieved 10- μm resolution in both axial and lateral dimensions but is limited to a penetration depth of several millimeters into biological tissues.

Because biological tissues are optically turbid media, light is quickly diffused inside tissues as a result of strong scattering. Light transmitted through tissues is classified into three categories: ballistic light, quasi-ballistic light, and diffuse light. Ballistic light experiences no scattering by tissue and travels straight through the tissue and hence carries direct imaging information. Quasi-ballistic light experiences minimal forward-directed scattering and carries some imaging information. Diffuse light follows tortuous paths and carries little direct imaging information and overshadows ballistic or quasi-ballistic light.

For breast tissue of a clinically useful thickness (5–10 cm), scattered light must be used to image breast cancers. We have demonstrated that for a 5-cm-thick breast tissue with the assumed absorption coefficient $\mu_a = 0.1 \text{ cm}^{-1}$ and reduced scattering coefficient $\mu_s' = 10 \text{ cm}^{-1}$, only the transmitted light that has experienced at least 1100 scattering events in tissue is able to yield enough signal.² Therefore ballistic light or even quasi-ballistic light does not exist for practical purposes. However, if a 10-mW visible or near-IR laser beam is incident upon a 5-cm-thick breast tissue, we estimate with diffusion theory that the diffuse transmittance is of the order of 10 nW/cm^2 or 10^{10} photons/(s cm^2), which is easy to

The authors are with the Optical Imaging Laboratory, Bioengineering Program, Texas A&M University, College Station, Texas 77843-3120.

Received 10 January 1997; revised manuscript received 19 May 1997.

0003-6935/97/287277-06\$10.00/0

© 1997 Optical Society of America

detect with a photomultiplier tube (PMT) capable of single-photon counting. The diffuse transmittance through a 10-cm-thick breast tissue would be similarly of the order of 1 pW/cm^2 or $10^6 \text{ photons/(s cm}^2)$.

To use the diffuse light for its abundance and to overcome its lack of direct imaging information, several researchers have studied ultrasound-modulated optical tomography of turbid media. Marks *et al.* investigated the combination of pulsed ultrasound and laser light and detected ultrasound-modulated optical signal in a homogeneous turbid medium without buried objects.³ Wang *et al.* developed ultrasound-modulated optical tomography that combined continuous-wave ultrasound and laser irradiation and successfully imaged buried objects in tissue-simulating turbid media.⁴ The major advantage of continuous-wave ultrasonic modulation over pulsed ultrasonic modulation was the significant increase in signal-to-noise ratio. Leutz and Maret reported the observation of ultrasonic modulation of multiply scattered light with an unfocused ultrasonic wave.⁵ Kempe *et al.* investigated the modulation of the optical field transmitted through a turbid medium by a quasi-continuous-wave ultrasound beam.⁶

We report the experimental results of our recent studies. The optical detector was moved away from the optic axis and the ultrasound-modulated optical signal was recorded to verify that ultrasound-modulated optical tomography depends on diffuse light as opposed to ballistic light. The ultrasound-modulated optical signal was compared with the unmodulated signal as the aperture in front of the optical detector varied in size. Two two-dimensional (2-D)-images of an object buried in a dense turbid medium were obtained with the ultrasound-modulated and unmodulated optical signals, respectively. The thickness of the dense media in transport mean free path was much greater than those previously reported.

2. Methods

We prepared liquid tissue phantoms (turbid media) to simulate the optical properties of tissues by dissolving dominantly absorbing Trypan blue dye and dominantly scattering Intralipid in water. We prepared gel tissue phantoms similarly by dissolving Trypan blue dye and Intralipid in 5% (by weight) gelatin solutions. We controlled the optical properties by varying the amounts of absorbers and scatterers independently. The scattering anisotropy of Intralipid at 632.8-nm wavelength was ~ 0.8 (Ref. 7). The phantom was contained in a 5-cm-thick cuvette. An ultrasonic absorber was placed at the bottom of the cuvette to avoid ultrasonic reflection.

To make a gel phantom that contains a buried object, a gelatin solution mixed with various amounts of dye and Intralipid was prepared in the cuvette before it was coagulated in a refrigerator. Another small gel phantom cube was placed inside the background gel in the midplane to simulate a buried tumor. The facets of the cube were parallel with those of the cuvette. A liquid phantom that had concen-

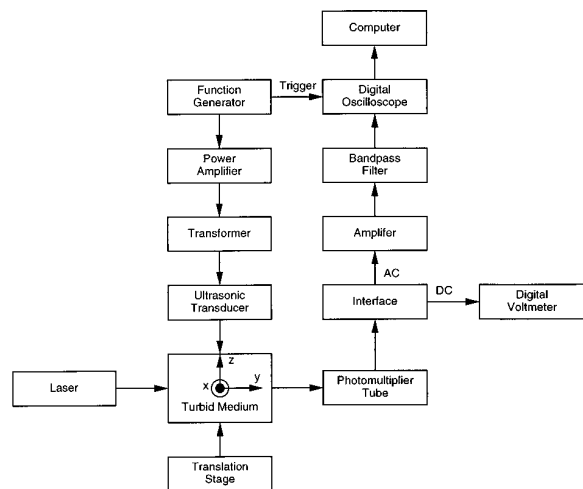


Fig. 1. Block diagram of the experimental setup.

trations of absorbers and scatterers identical to the background gel was poured into the cuvette to couple ultrasonic waves and to allow the scanning of ultrasonic transducers.

A block diagram of the experimental setup is shown in Fig. 1. The glass cuvette that contains turbid medium was seated on a 2-D translation stage. While the cuvette was translated to image the buried object, the rest of the system, including the optical and ultrasonic systems, was fixed.

A He-Ne laser with an output power of 10 mW and a wavelength of 632.8 nm delivered a single-mode Gaussian beam perpendicular to the front surface of the cuvette. The spot size of the laser beam on the incident surface of the medium was approximately 1 mm. The lower end of the ultrasonic transducer was buried in the liquid phantom to allow a good coupling of the ultrasonic wave. An aperture was placed in front of the PMT to control the amount of light that entered the PMT.

A function generator produced a sinusoidal wave at a fixed frequency of 1 MHz. This signal drove the ultrasonic transducer after it was amplified to 45-V amplitude by a power amplifier and a transformer.

The operating bandwidth of the ultrasonic transducer was centered at 1 MHz. The diameter of the active element of the ultrasonic transducer was 1.9 cm. The focal length of the transducer in water was 3.68 cm. The diameter of the ultrasonic focal spot in water was 0.29 cm. The acoustic wavelength in water was 0.15 cm.

After light passed through the aperture and reached the PMT, the optical signal was converted into an electrical signal while the ambient lights were turned off to reduce the ambient noise collected by the PMT. The electrical signal was separated into dc and ac components by an interface circuit. The dc voltage was read by a digital voltmeter, and the ac voltage was amplified and then effectively filtered by a narrow bandpass filter. The filtered signal was collected and averaged over multiple sweeps by the

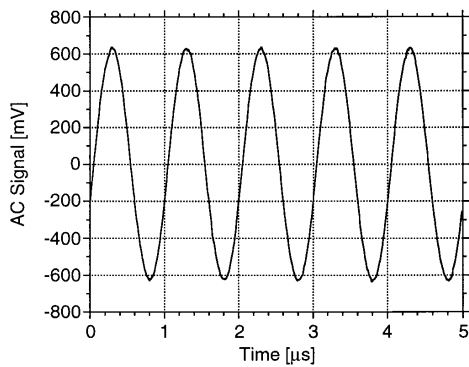


Fig. 2. Typical ac signal representing ultrasound-modulated optical signal.

digital oscilloscope, which was triggered by a reference signal from the function generator. Both the frequency filtering and the signal averaging enhanced the signal-to-noise ratio. The averaged time-domain signal was then transferred to a computer for data processing through a general-purpose interface bus connection. The peak-to-peak voltage of the ac signal represented the ultrasound-modulated optical signal, whereas the dc signal represented the unmodulated optical signal.

To study the dependence of the ac signal on the off-axis position of the PMT from the optic axis, we gradually translated the PMT detector away from the center and recorded the ac signal at each detector position. To investigate the dependence of the ac signal on the area of detection, we varied the size of the aperture in front of the PMT and recorded the ac signal along with the dc signal at each aperture size. To obtain a cross-sectional image of the turbid medium, the cuvette was translated in two dimensions and the ac and the dc signals were recorded at each position. Once the signals of all the scanned positions were obtained, images of the turbid medium that contained a buried object were constructed.

A Cartesian coordinate system was set up for convenience. The x axis was a horizontal axis perpendicular to the optic axis. The y axis was the optic axis defined by the laser beam. The z axis was the ultrasonic axis that was defined by the ultrasonic wave.

3. Results

A typical ac signal that represents an ultrasound-modulated optical signal obtained with a gel turbid medium is shown in Fig. 2. The optical properties of the 5-cm-thick homogeneous gel turbid medium included an absorption coefficient $\mu_a = 0.1 \text{ cm}^{-1}$ and a reduced scattering coefficient $\mu_s' = 10 \text{ cm}^{-1}$. The period of the sinusoidal function was $1 \mu\text{s}$, corresponding to the 1-MHz frequency of the ultrasonic wave.

The ac voltage was recorded for various PMT positions along the horizontal x axis (Fig. 3). The optical properties of the 5-cm-thick homogeneous liquid tur-

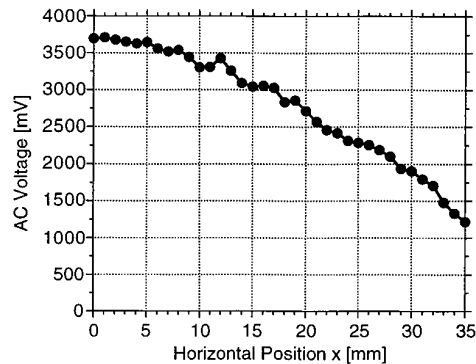


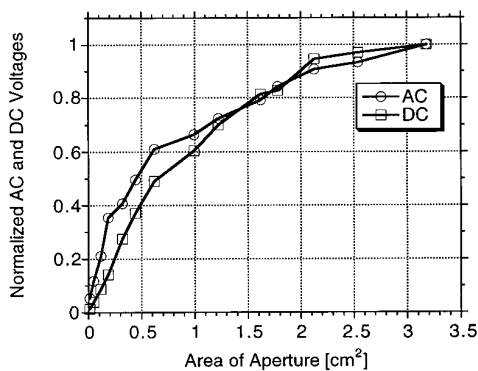
Fig. 3. Peak-to-peak ac voltage as a function of the horizontal position (x coordinate) of the PMT.

bid medium included an absorption coefficient $\mu_a = 0.1 \text{ cm}^{-1}$ and a reduced scattering coefficient $\mu_s' = 6.2 \text{ cm}^{-1}$. The aperture in front of the PMT was 2.1 cm in diameter. The PMT was first centered on the optic axis (y axis) and was then translated away from the optic axis with a 1-mm step size. We obtained the ac voltage at each PMT position by measuring its peak-to-peak voltage on the oscilloscope.

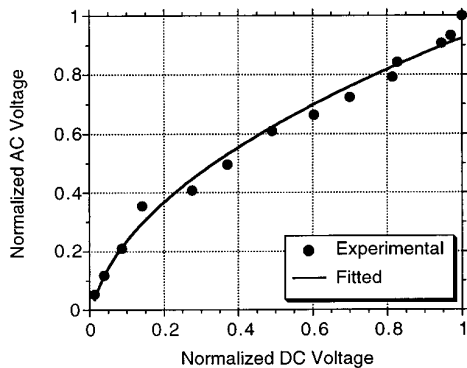
The aperture in front of the PMT was varied in diameter while the PMT was centered on the optic axis. Both the dc and the peak-to-peak ac voltages were recorded at each diameter. The optical properties of the 5-cm-thick homogeneous liquid turbid medium included an absorption coefficient $\mu_a = 0.1 \text{ cm}^{-1}$ and a reduced scattering coefficient $\mu_s' = 6.2 \text{ cm}^{-1}$. The normalized ac and dc signals were plotted as a function of the area of the aperture [Fig. 4(a)]. The ac signal was plotted as a function of the dc signal and was fitted with a square-root relationship with the dc signal [Fig. 4(b)].

We calculated the diffuse transmittance of a normal incident laser beam through a 5-cm-thick slab using diffusion theory for various values of detection area (Fig. 5).^{8,9} The optical properties of the homogeneous slab included an absorption coefficient $\mu_a = 0.1 \text{ cm}^{-1}$ and a reduced scattering coefficient $\mu_s' = 6.2 \text{ cm}^{-1}$. The incident laser beam had a diameter of 0.1 cm.

We obtained a 2-D image of an object buried in the middle plane of a turbid medium by raster scanning the turbid medium and recording the ac signal [Fig. 6(a)]. Both the buried object and the background medium were made of gels. The buried object was an approximately 5-mm-wide cube. The optical properties of the 5-cm-thick background turbid medium included an absorption coefficient $\mu_a = 0.1 \text{ cm}^{-1}$ and a reduced scattering coefficient $\mu_s' = 10 \text{ cm}^{-1}$. The thickness of the background turbid medium corresponded to ~ 50 transport mean free paths. The optical properties of the buried object included an absorption coefficient $\mu_a = 1.1 \text{ cm}^{-1}$ and a reduced scattering coefficient $\mu_s' = 10 \text{ cm}^{-1}$. In other words, the absorption coefficient of the buried object was 10 times greater than that of the background medium



(a)



(b)

Fig. 4. (a) Normalized ac and dc voltages as a function of the area of the aperture in front of the PMT; (b) normalized ac signal representing ultrasound-modulated optical signal as a function of the normalized dc signal representing unmodulated optical signal. A square-root fit was shown to model the experimental data.

while the reduced scattering coefficient of the buried object was the same as that of the background medium. The turbid medium was translated along the x and z axes with a 1-mm step size. The ultrasound-modulated optical signal (ac signal) was recorded at each position. A 2-D density plot was then gener-

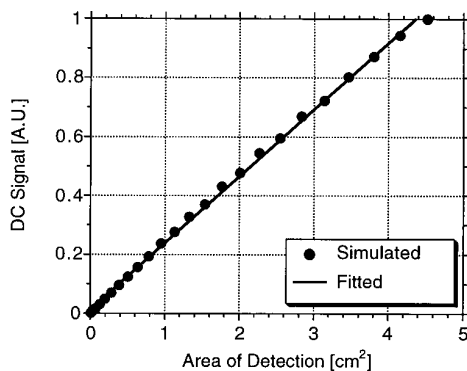
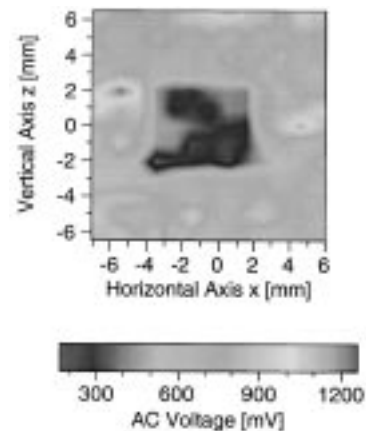
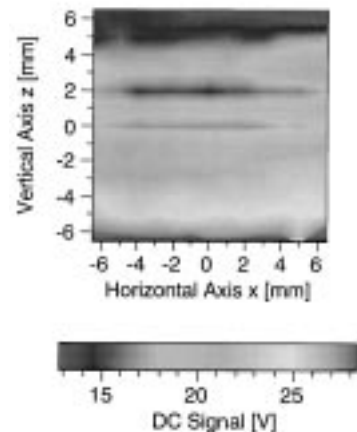


Fig. 5. Simulated relative dc signal as a function of the area of detection, based on diffusion theory. A linear fit was shown to model the experimental data.



(a)



(b)

Fig. 6. (a) 2-D ac image of an absorbing object buried in a 5-cm-thick dense turbid medium, using the ultrasound-modulated optical signal (ac signal); (b) 2-D attempted dc image of an absorbing object buried in a 5-cm-thick dense turbid medium, using the unmodulated optical signal (dc signal).

ated. The edge resolution of the 2-D image of the buried object was approximately 2 mm.

For comparison, a 2-D plot of the dc signal was generated as well [Fig. 6(b)]. The dc signal was recorded simultaneously with the ac signal while the turbid medium was translated. The buried object was not observable in the dc plot.

4. Conclusions and Discussion

Figure 2 showed the existence of ultrasonic modulation of transmitted light. When the ultrasonic wave was turned off, the ac signal was reduced to a noise level that was caused by the shot noise and the ambient noise. When the laser light was blocked and the ultrasonic wave was kept on, the ac signal was reduced to a noise level that was caused by the ambient noise. Therefore the AC signal must have been generated by the interactions between the ultrasonic wave and the laser light.

A typical value of the dc signal was measured at

approximately 30 V while the ac amplitude was measured at approximately 1000 mV. On the basis of the gains of the ac and the dc branches, the ratio between the ac and the dc powers of the light impinging on the PMT photocathode was estimated to be of the order of 10^{-6} – 10^{-5} , which was the modulation depth of the overall signal m . The modulation was weak for several reasons. The compressibility of the medium was of the order of $4.6 \times 10^{-5} \text{ bars}^{-1}$, and the peak pressure at the ultrasonic focus was approximately 2 bars. Hence, the volume compression was of the order of 10^{-4} . Some transmitted light bypassed the ultrasonic field with no modulation. The incoherent addition of multiple coherence areas on the detector was another factor that caused the low modulation depth.⁶

The diameter of each coherence area can be calculated with the expression $\phi_c = \lambda z / \phi_s$, where λ was the wavelength, z was the distance between the exit surface of the medium for scattered light and the detector, and ϕ_s was the effective diameter of the exit surface limited by the aperture placed in front of the PMT. The number of coherence areas covered by the PMT photocathode was $N = (\phi_d / \phi_c)^2$, where ϕ_d was the effective diameter of the PMT cathode. Using the experimental values in our setup, we estimated that there were of the order of 10^8 coherence areas detected, i.e., $N \approx 10^8$. Because N was proportional to the area of detection, the detected dc signal was proportional to N (Fig. 5), and the detected ac signal was proportional to the square root of N , i.e., \sqrt{N} (Fig. 4). The modulation depth of the overall detected signal m was related to the modulation depth of a single coherence area m_1 by $m = m_1 / \sqrt{N}$. Because m was 10^{-6} – 10^{-5} , the modulation depth of a single coherence area m_1 was estimated to be 0.01–0.1.

Figure 3 demonstrated that the ultrasound-modulated optical signal depended on diffuse light instead of ballistic light. If the ultrasound-modulated optical signal had depended on ballistic light, the signal would have disappeared when the PMT was moved away from the optic axis. The gradual decrease of the ac signal indicated that the ultrasound-modulated optical signal originated from the interactions between diffuse light and ultrasound.

Figure 4(a) showed that the dc signal increased nonlinearly with the aperture in front of the PMT. However, diffusion theory revealed that the dc signal was supposed to be proportional to the area of detection within limits (Fig. 5). The experimental nonlinearity was caused by the geometric coupling of light from the exit surface of the turbid medium to the photocathode of the PMT. The aperture had a distance from both the exit surface of the turbid medium and the photocathode of the PMT. The PMT housing may block some light, especially at large aperture sizes. Therefore the area of the aperture was not equal to or proportional to the area of detection of the PMT.

On the basis of the results in Fig. 5, the measured

dc signal was expected to be proportional to the area of detection. The ac signal was plotted against the dc signal [Fig. 4(b)]. A square root relationship between the ac and dc signals fitted very well.

Note that the dc signal should be proportional to the area of the detection only within limits. Because of conservation of energy, the dc signal was expected to reach a plateau when the area of detection reached a certain value. The transmittance decayed approximately exponentially as a function of the radial position, which ensured that the integration over the full plane of transmission converged.

The diffusion theory that was used to obtain the results in Fig. 5 did not account for coherence of light. The coherent light source in our experimental setup generated speckles on the detector surface, which was not modeled in the diffusion theory. However, the mean intensity of the speckles (dc signal) was expected to be identical with the simulated intensity, based on the diffusion theory.¹⁰

The possible mechanisms of ultrasonic modulation of light can be classified into three approaches: (1) direct intensity modulation, (2) scatterer-displacement modulation, and (3) photon-phonon interactions.¹¹ The direct intensity modulation was caused by the ultrasonic modulation of the optical properties of the turbid medium and did not require coherence of the light source. The ultrasonic wave caused a pressure variation in the medium. The pressure variation induced a density change in the medium as a result of the compressibility of the medium. The optical absorption and scattering coefficients were proportional to the number density of absorbers and scatterers, respectively. The index of refraction varied with the density as well. Therefore the density variation modulated the optical properties of the medium at the ultrasonic frequency. The variation of optical properties modulated the intensity of the light that passed through the ultrasonic field.

The scatterer-displacement modulation was a coherent speckle effect. The transmitted light had suffered multiple scattering events. The phase of the transmitted light depended on its path length. The ultrasonic field caused the scatterers to oscillate at the ultrasonic frequency and hence modulated the path length. The path-length variation modulated the speckle pattern, which led to an intensity variation on the PMT.^{5,6}

In the photon-phonon interactions approach, the light was considered as photons while the ultrasonic field was considered as phonons. The photon-phonon interactions caused the frequency of the light to shift by multiples of the ultrasonic frequency, which was Doppler shift in the classical sense.¹² The frequency-shifted light and unshifted light interfered on the PMT and yielded a component of the difference between the frequencies. The frequency shift was therefore converted into an intensity variation at the multiples of the ultrasonic frequency. The intensity variation at the fundamental frequency would be the strongest although the second harmonic component was experimentally observed previously.⁵

The question of which approach was dominant in our experiments is most important. Incoherent broadband light was used in place of laser light to examine the intensity modulation approach. No ultrasound-modulated optical signal was observed experimentally with the incoherence light source. This preliminary experiment discarded the direct intensity modulation approach because the direct intensity modulation approach did not require coherence of the light source and should have allowed us to observe an ultrasound-modulated optical signal if it was in play.

The photon-phonon interactions approach and the scatterer-displacement modulation approach may be merged into one approach if the ultrasonic modulation of the index of refraction is taken into account in the calculation of the optical path length. However, for clarity we considered the two approaches separately, and we hope to evaluate the relative contributions from each approach in the future. Both approaches involved observations of speckles and therefore required coherence of the light source. The ultrasound-modulated optical signal was expected to grow with the square root of the area of detection, assuming the coherence areas (speckle spots) were uncorrelated, which was experimentally confirmed as shown in Fig. 4(b). Further studies would reveal the relative importance of the two coherent approaches.

The buried object was clearly visible in the 2-D ac image [Fig. 6(a)]. The edge resolution in both the x and the z directions was approximately 2 mm. The lateral resolution in the x direction was due to the tight focus of the ultrasonic wave and the decrease of light fluence near and inside the absorbing object. No good explanation for the resolution in the z direction is yet available.

5. Summary

Ultrasonic modulation of scattered laser light was used to image absorbing objects buried in tissue-simulating turbid media. The buried object had 10 times greater absorption coefficient than the background turbid medium, whose optical properties included an absorption coefficient 0.1 cm^{-1} and a reduced scattering coefficient 10 cm^{-1} . We imaged buried objects in 5-cm-thick tissue phantoms with millimeter resolution by scanning and detecting alterations of the ultrasound-modulated optical signal. It was experimentally proved that ultrasound-

modulated optical tomography depended on diffuse light instead of ballistic light. Coherent approaches were the dominant mechanisms of ultrasonic modulation of light in our experiments on dense turbid media.

This project was sponsored in part by the National Institutes of Health grant R29 CA68562 and The Whitaker Foundation.

References

1. See related studies in R. R. Alfano and J. G. Fujimoto, eds., *Advances in Optical Imaging and Photon Migration*, Vol. 2 of Trends in Optics and Photonics Series (Optical Society of America, Washington, D.C., 1996).
2. L. Wang and S. L. Jacques, "Application of probability of n scatterings of light passing through an idealized tissue slab in breast imaging," in *Advances in Optical Imaging and Photon Migration*, R. R. Alfano, ed., Vol. 21 of OSA Proceedings Series (Optical Society of America, Washington, D.C., 1994), pp. 181–186.
3. F. A. Marks, H. W. Tomlinson, and G. W. Brooksby, "Comprehensive approach to breast cancer detection using light: photon localization by ultrasound modulation and tissue characterization by spectral discrimination," in *Photon Migration and Imaging in Random Media and Tissues*, B. Chance and R. R. Alfano, eds., Proc. SPIE **1888**, 500–510 (1993).
4. L. Wang, S. L. Jacques, and X. Zhao, "Continuous-wave ultrasonic modulation of scattered laser light to image objects in turbid media," *Opt. Lett.* **20**, 629–631 (1995).
5. W. Leutz and G. Maret, "Ultrasonic modulation of multiply scattered light," *Physica B* **204**, 14–19 (1995).
6. M. Kempe, M. Larionov, D. Zaslavsky, and A. Z. Genack, "Acousto-optic tomography with multiply scattered light," *J. Opt. Soc. Am. A* **14**, 1151–1158 (1997).
7. S. T. Flock, S. L. Jacques, B. C. Wilson, W. M. Star, and M. J. van Gemert, "Optical properties of Intralipid: a phantom medium for light propagation studies," *Lasers Surg. Med.* **12**, 510–519 (1992).
8. T. J. Farrell, M. S. Patterson, and B. C. Wilson, "A diffusion theory model of spatially resolved, steady-state diffuse reflectance for the noninvasive determination of tissue optical properties *in vivo*," *Med. Phys.* **19**, 879–888 (1992).
9. L.-H. Wang, X. Zhao, and S. L. Jacques, "Computation of the optical properties of tissues from light reflectance using a neural network," in *Laser-Tissue Interaction V*, S. L. Jacques, ed., Proc. SPIE **2134A**, 391–399 (1994).
10. J. W. Goodman, *Statistical Optics* (Wiley, New York, 1985).
11. L. Wang, X. Zhao, and S. L. Jacques, "Ultrasound-modulated optical tomography for thick tissue imaging," in *Photon Propagation in Tissues*, B. Chance, D. T. Delpy, and G. J. Mueller, eds., Proc. SPIE **2626**, 237–248 (1995).
12. A. Korpel, *Acousto-Optics* (Marcel Dekker, New York, 1988).